Scientific Research Publishing

Computational Molecular Bioscience, 2023, 13, 63-74
https://www.scirp.org/journal/cmb
ISSN Online: 2165-3453
ISSN Print: 2165-3445

A Computational Study of Microhydrated N-Acetyl-Phenylalaninylamide (NAPA): Kinetics and Thermodynamics

Mohammad Alauddin[1*], Mohammad Masud Parvez[2], Mohammad Abdul Matin[3]

[1]Department of Theoretical and Computational Chemistry, University of Dhaka, Dhaka, Bangladesh
[2]Department of Chemistry, University of Barishal, Barishal, Bangladesh
[3]Centre for Advanced Research in Sciences (CARS), University of Dhaka, Dhaka, Bangladesh
Email: *alauddin1982@du.ac.bd

How to cite this paper: Alauddin, M., Parvez, M.M. and Matin, M.A. (2023) A Computational Study of Microhydrated N-Acetyl-Phenylalaninylamide (NAPA): Kinetics and Thermodynamics. *Computational Molecular Bioscience*, **13**, 63-74.
https://doi.org/10.4236/cmb.2023.134005

Received: September 21, 2023
Accepted: December 10, 2023
Published: December 13, 2023

Copyright © 2023 by author(s) and Scientific Research Publishing Inc.
This work is licensed under the Creative Commons Attribution International License (CC BY 4.0).
http://creativecommons.org/licenses/by/4.0/

Open Access

Abstract

The formations of [NAPA-A$(H_2O)_n$ (n = 1, 2, 3, 4)] complexes have been studied employing DFT/*w*B97XD/cc-pVTZ computational level to understand the kinetics and thermodynamics for the hydration reactions of N-acetyl-phenylalaninylamide (NAPA). Thermodynamic parameters such as reaction energy (E), enthalpy (H), Gibb's free energy (G), specific heat capacity (C_v), entropy (S), and change of these parameters (ΔE_r, ΔH_r, ΔG_r, ΔC_r, and ΔS_r) were studied using the explicit solvent model. The predicted values of H, G, C, and S increase with the sequential addition of water in NAPA-A due to the increase in the total number of vibrational modes. On the other hand, the value of ΔE_r, ΔH_r, and ΔG_r increases (more negative to less negative) gradually for n = 1, 2, 3, and 4 that indicates an increase of hydration in NAPA-A makes exothermic to endothermic reactions. The barrier heights for the transition states (TS) of [NAPA-A$(H_2O)_n$ (n = 1, 2, 3, 4)] complexes are predicted to lie at 4.41, 4.05, 3.72 and 2.26 kcal/mol respectively below the reactants. According to the calculations, the formations of [NAPA-A$(H_2O)_1$] and [NAPA-A$(H_2O)_2$] complexes are barrierless reactions because both water molecules are strongly bonded via two hydrogen bonds in the backbone of NAPA-A. On the contrary, the reactions of [NAPA-A$(H_2O)_3$] and [NAPA-A$(H_2O)_4$] complexation are endothermic and the barrier heights are predicted to stay at 6.30 and 10.54 kcal/mol respectively above the reactants. The free energy of activation ($\Delta^{\ddagger}G^{\circ}$) for the reaction of [NAPA-A$(H_2O)_1$], [NAPA-A$(H_2O)_2$], [NAPA-A$(H_2O)_3$], and [NAPA-A$(H_2O)_4$] complexation are 4.43, 4.28, 3.83 and 5.11 kcal/mol respectively which are very low. As well as the rates of reactions are 3.490×10^9 s^{-1}, 4.514×10^9 s^{-1}, 9.688×10^9 s^{-1}, and 1.108×10^9 s^{-1} respectively which are very fast and spontaneous.

Keywords

Microhydration, DFT, Transition States, Kinetics, Thermodynamics

1. Introduction

Water plays a significant role in changing the structural, kinetic, and thermodynamic properties of peptides, proteins, nucleic acids, lipids, carbohydrates, and natural products [1] [2] [3] [4]. As well as regulates the biological activities of such biomolecules [5] [6]. However, it is still unknown how water molecules control the structures and biological functions. Therefore, it becomes a challenging issue in biophysical science from the experimental and theoretical points of view and also becomes a promising research era in which the aim is to understand the physicochemical properties and biological/pharmaceutical activities at the molecular level. Experimentally it is very difficult to understand the working mechanism due to the extremely rapid phenomena occurring in the bulk water as well as in the biomolecule-water interface. Nevertheless, some experimental techniques have been developed to study the biomolecule-water interface and reported that the molecules are more tightly connected in the interface than in the bulk and hence, fluctuations occur slowly in the interface [7] [8].

In contrast, computational approaches to biomolecule-water systems have been of great importance to the experimental society because of complementary and independent information to accurately interpret the nature of biomolecule-water interactions. Several experimental [9] [10] [11] [12] and theoretical [13] [14] [15] researches have been performed to interpret the structural, thermodynamic, and kinetic behavior of biomolecule-water interactions using explicit and implicit solvent models. Recently, Lanza *et al.* reported by comparing and analyzing the computed thermodynamics data of $Ala_3H^+{\cdot}22H_2O$ and $Val_3H^+{\cdot}22H_2O$ clusters that the β-strand structure of $Val_3H^+{\cdot}22H_2O$ clusters is more stable than $Ala_3H^+{\cdot}22H_2O$ clusters due to the hydration enthalpy and entropy [16]. Arsiccio *et al.* reported that they used a novel computational approach to study protein unfolding using pressure in an implicit solvent model and found that the volume reduction of the bound water is the key energetic factor for the denaturation of proteins under the effect of pressure [17]. Lanza *et al.* reported by computationally studying $AcAlaNH_2{\cdot}nH_2O$ (n = 1 - 13) complexes with the peptide in the fully extended (FE) conformation that the interaction energy increases upon increasing the number of water molecules [2]. Fischer *et al.* recently reported on the reaction of protonated triglycine (Gly_3H^+) with a single water molecule in the gas phase both experimentally and theoretically [18]. The highest barrier height of the transition state (TS) for cis isomer is computed to lie at 1.8 kJ/mol below the reactants. On the contrary, the highest barrier height of the TS for trans-isomer is found to lie 7.0 kJ/mol below the reactants.

The studies of kinetics and thermodynamics of peptide-water interactions are

focused on intermediate states (transition states), intermolecular interactions (cooperative hydrogen bonding), and free energy barriers [19]. The addition of water molecules in proteins, protein-ligand interfaces, protein-drug interfaces, or biopolymers modulates thermodynamic properties such as enthalpy, entropy, and Gibb's free energy depending on the number of hydrogen bond presence [20] [21]. As Gibb's free energy of activation depends on enthalpy and entropy [22], therefore, the addition of water in peptides or proteins changes the free energy of activation and finally changes the rate of reaction. In this manuscript, we studied the kinetics and thermodynamic properties of N-acetyl-phenylalaninylamide (NAPA) which is a model dipeptide, and its microhydration using the explicit solvent model in the gas phase.

2. Computational Details

The conformational analysis of NAPA was explored with the aid of AMBER force field [23] implemented in the HyperChem professional 7.51 package [24]. The structure of reactants (R), transition states (TS), and products (P) were computed employing density functional theory (DFT) calculations. The DFT computations were implemented at dispersion correction functional (*w*B97XD) in conjunction with the cc-pVTZ basis set in the gas phase. Vibrational frequency analyses were performed for the minimum energy structures to evaluate the character of stationary points and also to obtain zero-point vibration energy (ZPVE). The characteristics of local minima for reactants and products were proved by ascertaining that the second derivatives energy of matrices (Hessian) have no imaginary frequency. Transition state geometries were found by QST3 (quadratic synchronous transit-guided quasi-Newton approach) method and confirmed that Hessian matrices have an imaginary frequency. Thermal corrections were done to get thermochemical energies such as enthalpies and free energies at 298.15 K under atmospheric pressure. The IRC calculations were also performed using the same level of computational approach for all the transition states (TS) to prove whether these TS are associated between the reactants and products to the accurate minima or not. Total calculations were done with the aid of Gaussian16 computational program [25] and *GaussView* 6.0 was applied to visualize the geometry of the compounds. The rate of the reaction was calculated by renowned transition-state theory (TST) [26] via the below-mentioned equation:

$$k(T) = \frac{k_B T}{hc^0} e^{-\Delta^{\ddagger} G^0 / RT}$$

where $k(T)$ is the rate of reaction at temperature T, k_B is the Boltzmann constant (=1.380662 × 10^{-23} J/K), h is the Planck's constant (=6.627176 × 10^{-34} J·s), R is the gas constant (=8.31441 J/mol·K), c^0 is the standard concentration (=1 mol/L), and $\Delta^{\ddagger} G^0$ is Gibb's free energy of activation.

3. Results and Discussion

3.1. Geometry Optimization and Thermodynamic Stability

By applying MP2/6-31 + G* and DFT/*w*B97XD/cc-pVTZ computational levels,

N-acetyl-phenylalaninylamide (NAPA) molecules can assume four different conformations and they are NAPA-A, -B, -C, and -D. Among them, the minimum energy conformer is NAPA-A with the structural motif of β_L(a) and that is proved both experimentally as well as theoretically [27] [28] [29] [30] [31]. To avoid complexation, only NAPA-A conformer has been taken for microhydration. Several conformers are calculated for mono-, di-, tri-, and tetra-hydrated NAPA-A complexes using DFT/*w*B97XD/cc-pVTZ computational approach. The most stable conformers for all the hydrated NAPA complexes are taken into account for kinetics and thermochemical analysis in the gas phase. **Figure 1** shows the most stable structures of NAPA-A and its hydrated cluster. The Gaussian 16.0 program package is utilized to carry out thermochemical analysis at the default temperature (298.15 K) and pressure (1 atmosphere). All the thermodynamical parameters of hydrated NAPA-A complexes are computed and presented in **Table 1**.

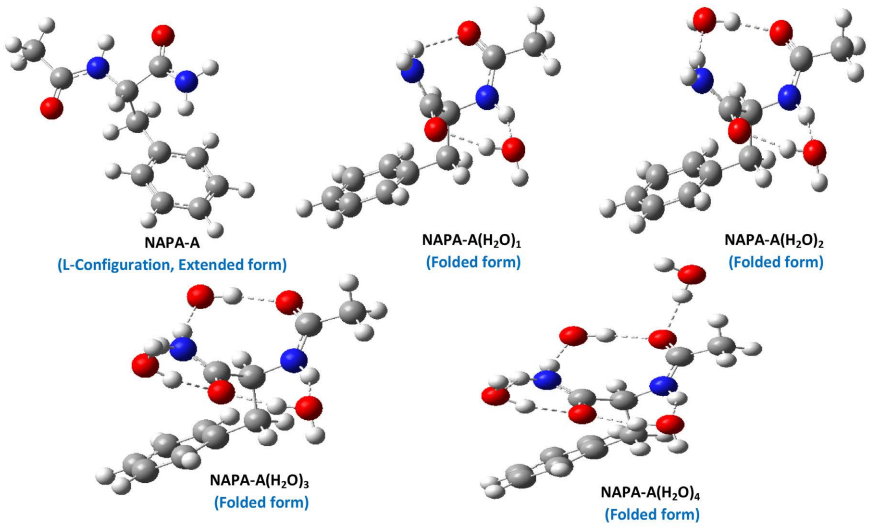

Figure 1. DFT-optimized the most stable structures of [NAPA-A(H_2O)$_n$ (n = 1, 2, 3, 4)] complexes.

Table 1. Calculated thermodynamic parameters of the most stable structures of NAPA-A, water and [NAPA-A(H_2O)$_n$ (n = 1, 2, 3, 4)] complexes with *w*B97XD/cc-pVTZ computational approach.

Molecule	E_0 (a.u.)	E_{ZPE} (a.u.)	$E_0 + E_{ZPE}$ (a.u.)	$E_0 + E_{Corr}$ (a.u.)	$E_0 + H_{Corr}$ (a.u.)	$E_0 + G_{Corr}$ (a.u.)	H	G	C	S
NAPA-A	−687.62464	0.24178	−687.38286	−687.36815	−687.36720	−687.42672	160.952	124.195	54.414	125.263
H_2O	−76.43483	0.02170	−76.41312	−76.41029	−76.40934	−76.43075	15.401	2.560	6.006	45.056
[NAPA-A(H_2O)$_1$]	−764.07833	0.26753	−763.81079	−763.79321	−763.79227	−763.85831	178.911	138.057	63.492	138.993
[NAPA-A(H_2O)$_2$]	−840.53763	0.29381	−840.24382	−840.22386	−840.22291	−840.29362	196.898	153.117	71.969	148.810
[NAPA-A(H_2O)$_3$]	−916.98901	0.31909	−916.66991	−916.64690	−916.64596	−916.72424	214.672	166.138	81.407	164.756
[NAPA-A(H_2O)$_4$]	−993.43648	0.34390	−993.09257	−993.06624	−993.06530	−993.15202	232.328	178.500	91.584	182.521

H = Enthalpy (kcal/mol), G = Gibb's free energy (kcal/mol), C = Heat Capacity (cal/mol-Kelvin) and S = Entropy (cal/mol-Kelvin).

The total energy for a molecular system is assumed by $E_{total} = E_0 + E_{vibrational} + E_{rotational} + E_{translational}$, where E_0 is the sum of $E_{electronic}$ and ZPE. This ZPE to the electronic energy considers for the effect of vibrations occurring even at 0 K in the molecule. Therefore, zero point corrected vibrational energy E, enthalpy H (H = E + RT), and Gibb's free energy G (G = H − TS) are accounted for the thermal correction. The values of H, G, $C_{v,}$ and S of NAPA-A are 160.952, 124.195, 54.414, and 125.263 in the respective units mentioned in Table 1. Successive addition of water molecules in NAPA-A increases the value of H, G, $C_{v,}$ and S at an almost constant rate. The total number of vibrational modes increases with the addition of water molecules. Ultimately the total electronic energies of [NAPA-A$(H_2O)_n$ (n = 1 - 4)] complexes are increased and therefore enthalpy, Gibb's free energy, heat capacity, and entropy increase.

3.2. Formation of Hydrated NAPA-A Complex and Thermochemical Analysis

The energy of a reaction is a very important parameter to understand the nature of the reaction. The reaction for the formation of [NAPA-A$(H_2O)_n$] complexes are given below:

$$\text{NAPA-A} + (H_2O)_n\ (n = 1, 2, 3, 4) \rightarrow [\text{NAPA-A}(H_2O)_n\ (n = 1, 2, 3, 4)] \quad (1)$$

The energy of the reaction can be calculated by subtracting the total electronic energies of the bare NAPA-A and isolated water from the total electronic energy of [NAPA-A$(H_2O)_n$ (n = 1, 2, 3, 4)] complex. The equations for the calculation of the reaction energy (ΔE_r), the change of enthalpy (ΔH_r), the change of Gibb's free energy (ΔG_r), the change of heat capacity (ΔC_r) and the change of entropy (ΔS_r) are shown below:

ΔE_r = E[NAPA-A$(H_2O)_n$ (n = 1, 2, 3, 4)] − E[bare NAPA-A] − E[$(H_2O)_n$ (n = 1, 2, 3, 4)]

ΔH_r = H[NAPA-A$(H_2O)_n$ (n = 1, 2, 3, 4)] − H[bare NAPA-A] − H[$(H_2O)_n$ (n = 1, 2, 3, 4)]

ΔG_r = G[NAPA-A$(H_2O)_n$ (n = 1, 2, 3, 4)] − G[bare NAPA-A] − G[$(H_2O)_n$ (n = 1, 2, 3, 4)]

ΔC_r = C[NAPA-A$(H_2O)_n$ (n = 1, 2, 3, 4)] − C[bare NAPA-A] − C[$(H_2O)_n$ (n = 1, 2, 3, 4)]

ΔS_r = S[NAPA-A$(H_2O)_n$ (n = 1, 2, 3, 4)] − S[bare NAPA-A] − S[$(H_2O)_n$ (n = 1, 2, 3, 4)]

To calculate ΔE_r, ΔH_r, ΔG_r, ΔC_r, and ΔS_r the structures of reactants and products are very important. The structures of reactants, TS, and products are optimized using DFT/*w*B97XD/cc-pVTZ computational approach and are presented in Figure 2. The TS structures were confirmed by checking the Hessian matrices that have an imaginary frequency. The DFT-calculated ΔE_r, ΔH_r, ΔG_r, ΔC_r, and ΔS_r are summarized in Table 2. The values of ΔE_r, $\Delta H_{r,}$ and ΔS_r are negative (−) which means the formation of [NAPA-A$(H_2O)_n$ (n = 1, 2, 3, 4)] complexes from NAPA-A, [NAPA-A$(H_2O)_n$ (n = 1, 2, 3)] and H_2O are exothermic. In the formation

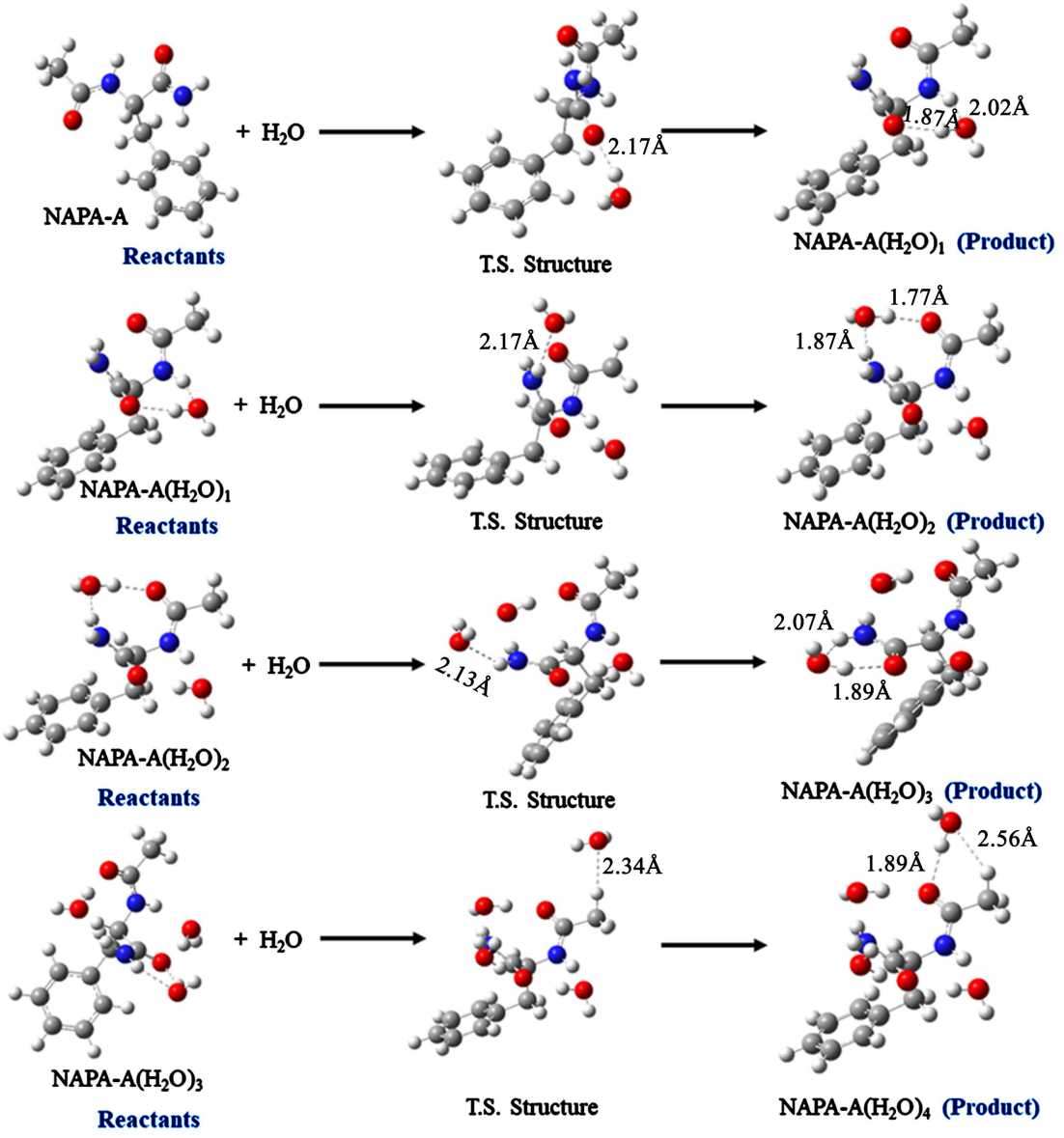

Figure 2. DFT-optimized the most stable structure of NAPA-A, transition state structures of [NAPA-A$(H_2O)_n$ (n = 1, 2, 3, 4)] complexes, and the most stable structure of [NAPA $(H_2O)_n$ (n = 1, 2, 3, 4)] complexes.

Table 2. DFT-calculated energy, enthalpy, Gibb's free energy, change of heat capacity, and entropy change for the reactions of NAPA-A and [NAPA-A$(H_2O)_n$ (n = 1, 2, 3)] complexes with water.

Reactions	ΔE_r (kcal/mol)	ΔH_r (kcal/mol)	ΔG_r (kcal/mol)	ΔC_r (kcal/mol-Kelvin)	ΔS_r (kcal/mol-Kelvin)
NAPA-A + H_2O → [NAPA-A$(H_2O)_1$]	−9.27	−9.87	−0.52	0.0030	−0.0313
[NAPA-A$(H_2O)_1$] + H_2O → [NAPA-A$(H_2O)_2$]	−12.77	−13.36	−2.86	0.0025	−0.0352
[NAPA-A$(H_2O)_2$] + H_2O → [NAPA-A$(H_2O)_3$]	−8.00	−8.60	0.08	0.0034	−0.0291
[NAPA-A$(H_2O)_3$] + H_2O → [NAPA-A$(H_2O)_4$]	−5.68	−6.27	1.86	0.0041	−0.0272

ΔE_r = Reaction energy, ΔH_r = Enthalpy of reaction, ΔG_r = Gibb's free energy of reaction, ΔC_r = Change of heat capacity and ΔS_r = Change of Entropy.

of [NAPA-A(H_2O)$_2$] complex, the values of ΔE_r, ΔH_r, and ΔS_r are more negative (−) compared to the other complexes' formation. Because the most stable conformer of [NAPA-A(H_2O)$_2$] complex has a structure that blocks both C_5 and C_7 backbone interactions by two water molecules which makes the complex more compact than others. The values of ΔE_r, ΔH_r, ΔG_r, ΔC_r, and ΔS_r for n = 1, 3, and 4 complexes are increased (more negative to more positive) as the total number of vibrational modes increases. The change ΔH_r, ΔG_r, ΔC_r, ΔS_r and the reaction energy (ΔE_r) for the successive addition of water molecule is depicted in **Figure 3**.

3.3. The Barrierless Reactions and Kinetics

Calculated energy of transition states, free energy of activation, and rate of the reaction for the reactions of NAPA-A and [NAPA-A(H_2O)$_n$ (n = 1, 2, 3)] complexes with water are shown in **Table 3**. A sketch of the calculated potential energy surface (PES) with DFT/*ω*B97XD/cc-pVTZ computational approach for the NAPA-A + (H_2O)$_n$ (n = 1, 2, 3, 4) → [NAPA-A(H_2O)$_n$ (n = 1, 2, 3, 4)] are shown in **Figure 4** and the structures of reactants, TS and products are presented in **Figure 2**. Transition state geometries were obtained by QST3 method and were confirmed that Hessian matrices have an imaginary frequency. Transition state complexes have longer hydrogen bond distances than the stable [NAPA-A(H_2O)$_n$ (n = 1, 2, 3, 4)] complexes (products) (**Figure 2**).

It is very interesting that the barrier height for the transition states (TS) of [NAPA-A(H_2O)$_n$ (n = 1, 2, 3, 4)] complexes are computed to lie at 4.41, 4.05, 3.72, and 2.26 kcal/mol below the reactants.

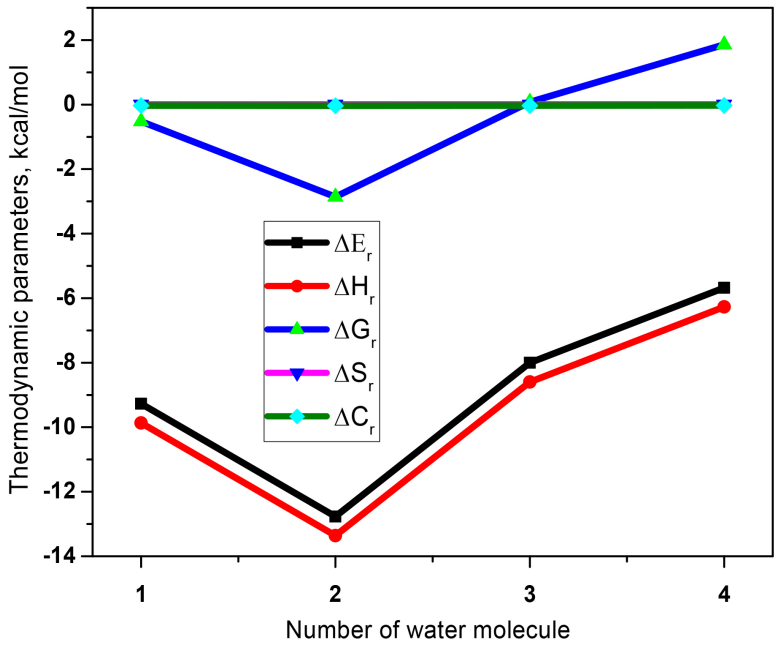

Figure 3. Graphs representing reaction energy, the change of enthalpy, the change of Gibb's free energy, the change of heat capacity and the change of entropy for the successive addition of water.

Table 3. Calculated energy of transition states, free energy of activation, and rate of the reaction for the reactions of NAPA-A and [NAPA-A(H_2O)$_n$ (n = 1, 2, 3)] complexes with water.

Reactions	Energy of the transition state (TS) structure (a.u.)	Free energy of activation, $\Delta^{\ddagger}G^{0}$ (kcal/mol)	Rate of the reaction, k (s^{-1})
NAPA-A + H_2O → [NAPA-A(H_2O)$_1$]	−763.803004	4.433355	3.490×10^{9}
[NAPA-A(H_2O)$_1$] + H_2O → [NAPA-A(H_2O)$_2$]	−840.229839	4.281497	4.514×10^{9}
[NAPA-A(H_2O)$_2$] + H_2O → [NAPA-A(H_2O)$_3$]	−916.663401	3.829062	9.688×10^{9}
[NAPA-A(H_2O)$_3$] + H_2O → [NAPA-A(H_2O)$_4$]	−993.086625	5.113575	1.108×10^{9}

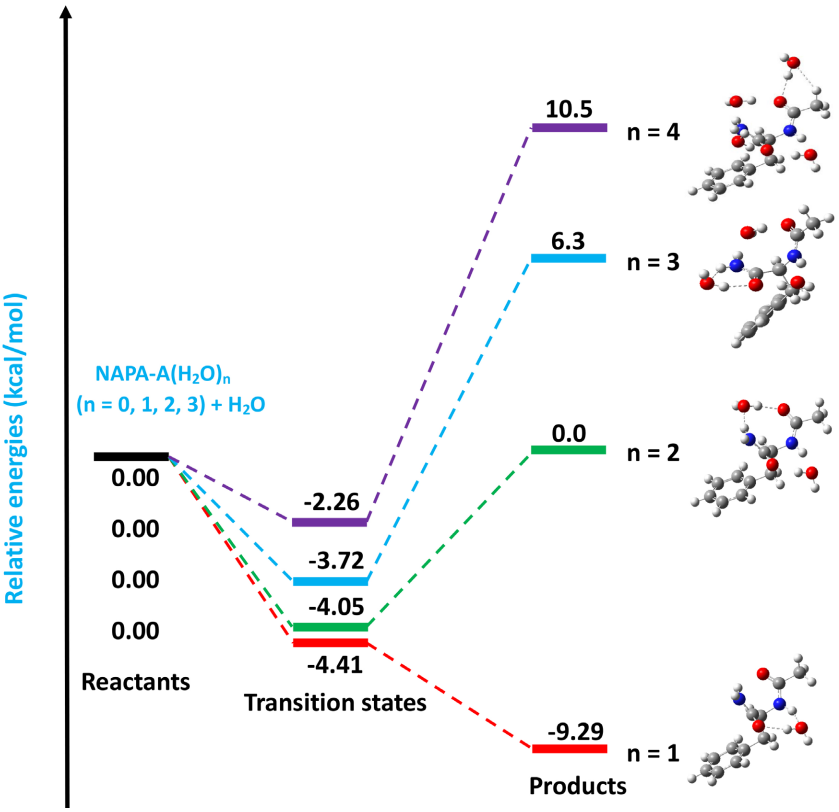

Figure 4. Potential energy surface (PES) for the reactions of NAPA-A and [NAPA-A(H_2O)$_n$ (n = 1, 2, 3)] complexes with water having no energy barrier. Relative energies are given in kcal/mol.

Consequently, the barrier height for the production of the stable complex of [NAPA-A(H_2O)$_1$] is found to lie 9.29 kcal/mol below the reactants, and for [NAPA-A(H_2O)$_2$] complex is computed to lie 0.03 kcal/mol above the reactants. These calculated results confirmed that the products formed global minima [32]. The NAPA-A conformer has both C_5 and C_7 backbone interaction positions. For the 1st reaction NAPA-A + (H_2O)$_1$ → [NAPA-A(H_2O)$_1$] complex, where water molecule goes C_5 interactions position and formed very stable complex and for the 2nd reaction [NAPA-A(H_2O)$_1$] + (H_2O)$_1$ → [NAPA-A(H_2O)$_2$] complex, where water molecule goes C_7 interactions position and formed very stable complex.

As water molecules are strongly bonded via two hydrogen bonds, the value of entropy is more negative compared to the higher cluster and therefore these two reactions are barrierless [33].

On the other hand, the 3rd reaction [NAPA-A(H_2O)$_2$] + (H_2O)$_1$ → [NAPA-A(H_2O)$_3$] complex and the 4th reaction [NAPA-A(H_2O)$_3$] + (H_2O)$_1$ → [NAPA-A(H_2O)$_4$] complex, the 3rd and 4th water molecule are not directly connected to the backbone of NAPA-A. That means these two water molecules are loosely bound to NAPA-A and hence entropy value is less negative compared to 1st and 2nd complexes. Due to the increase of entropy, the 3rd and 4th reactions are endothermic, and the barrier heights are predicted to lie at 6.30 and 10.54 kcal/mol above the reactants. To understand the kinetic behaviors, Gibb's free energy of activation ($\Delta^{\ddagger}G^{o}$) as well as the rate of reaction (k) have been calculated for all the reactions. The calculated values of $\Delta^{\ddagger}G^{o}$ are 4.43, 4.28, 3.83, and 5.11 kcal/mol for 1st, 2nd, 3rd, and 4th reactions respectively. Finally, the rate of reactions is 3.490 × 10^9, 4.514 × 10^9, 9.688 × 10^9, and 1.108 × 10^9 per second for 1st, 2nd, 3rd and 4th reactions respectively. That means all the reactions are very fast but the formation of trihydrated NAPA-A complex from dihydrated NAPA-A and water is faster than other hydrated complex formation reactions.

4. Conclusion

In this work, we studied the thermodynamics and kinetics of N-acetyl-phenylalaninylamide (NAPA) and its microhydration using the explicit solvent model in the gas phase. The most stable conformers of [NAPA-A(H_2O)$_n$ (n = 0 - 4)] complexes are taken into account for kinetics and thermochemical analysis. The values of H, G, C_v, and S of NAPA-A and its hydrated complexes increase with the successive addition of water molecules due to the increase in the total number of vibrational modes. On the other hand, the values of ΔE_r, ΔH_r, and ΔG_r become more negative to less negative which indicates the sequential addition of water in NAPA-A makes exothermic to endothermic reactions. Transition state geometries were calculated by the QST3 method and the barrier height for the transition states (TS) of [NAPA-A(H_2O)$_n$ (n = 1, 2, 3, 4)] complexes are predicted to lie 4.41, 4.05, 3.72 and 2.26 kcal/mol below the reactants. According to our calculations, the first two reactions means the formation of [NAPA-A(H_2O)$_1$] and [NAPA-A(H_2O)$_2$] complexes are barrierless reactions because both water molecules are strongly bonded via two hydrogen bonding in the backbone of NAPA-A peptide. Whereas [NAPA-A(H_2O)$_3$] and [NAPA-A(H_2O)$_4$] complex formation reactions are endothermic and the barrier heights are calculated to lie at 6.30 and 10.54 kcal/mol respectively above the reactants. To see the kinetic effect, we calculated the rate of reactions for the formation of [NAPA-A(H_2O)$_1$], [NAPA-A(H_2O)$_2$], [NAPA-A(H_2O)$_3$], and [NAPA-A(H_2O)$_4$] complexes are 3.490 × 10^9 s^{-1}, 4.514 × 10^9 s^{-1}, 9.688 × 10^9 s^{-1} and 1.108 × 10^9 s^{-1} respectively. This theoretical observation messages us that the microhydration of NAPA-A is very fast and spontaneous.

Data Availability

All generated data is available from the authors under request.

Conflicts of Interest

The authors declare that there is no conflict of financial interests.

References

[1] Schweitzer-Stenner, R. (2012) Protein and Peptide Folding, Misfolding and Non-Folding. Wiley, Hoboken.

[2] Lanza, G. and Chiacchio, M.A. (2014) Ab Initio MP2 and Density Functional Theory Computational Study of $AcAlaNH_2$ Peptide Hydration: A Bottom-Up Approach. *ChemPhysChem*, **15**, 2785-2793. https://doi.org/10.1002/cphc.201402222

[3] Young, T., Abel, R., Kim, B., Berne, B.J. and Friesner, R.A. (2007) Motifs for Molecular Recognition Exploiting Hydrophobic Enclosure in Protein-Ligand Binding. *Proceedings of the National Academy of Sciences of the United States of America*, **104**, 808-813. https://doi.org/10.1073/pnas.0610202104

[4] Fuchs, P.F.J., Bonvin, A.M.J.J., Bochicchio, B., Pepe, A., Alix, A.J.P. and Tamburro, A.M. (2006) Kinetics and Thermodynamics of Type VIII β-Turn Formation: A CD, NMR, and Microsecond Explicit Molecular Dynamics Study of the GDNP Tetrapeptide. *Biophysical Journal*, **90**, 2745-2759. https://doi.org/10.1529/biophysj.105.074401

[5] Schiebel, J., Gaspari, R., Wulsdorf, T., Ngo, K., Sohn, C., Schrader, A., Cavalli, A., Ostermann, T.E., Heine, A. and Klebe, G. (2018) Intriguing Role of Water in Protein-Ligand Binding Studied by Neutron Crystallography on Trypsin Complexes. *Nature Communications*, **9**, Article No. 3559. https://doi.org/10.1038/s41467-018-05769-2

[6] Hilser, V.J. (2011) Finding the Wet Spots, *Nature*, **469**, 166-167. https://doi.org/10.1038/469166a

[7] Hua, W., Ai, Y.J., Gao, B., Li, H., Agren, H. and Luo, Y. (2012) X-Ray Spectroscopy of Blocked Alanine in Water Solution from Supermolecular and Supermolecular-Continuum Solvation Models: A First-Principles Study. *Physical Chemistry Chemical Physics*, **14**, 9666-9675. https://doi.org/10.1039/c2cp40732a

[8] Comez, L., Lupi, L., Morresi, A., Paolantoni, M., Sassi, P. and Fioretto, D. (2013) More Is Different: Experimental Results on the Effect of Biomolecules on the Dynamics of Hydration Water. *Journal of Physical Chemistry Letters*, **4**, 1188-1192. https://doi.org/10.1021/jz400360v

[9] Vraneŝ, M., Paniĉ, J., Tot, A., Papoviĉ, S., Gadžurić, S., Podlipnik, Ĉ. and Beŝter-Rogaĉ, M. (2021) From Amino Acids to Dipeptide: The Changes in Thermal Stability and Hydration Properties of β-Alanine, L-Histidine and L-Carnosine. *Journal of Molecular Liquids*, **328**, Article ID: 115250. https://doi.org/10.1016/j.molliq.2020.115250

[10] Gavrilov, Y., Leuchter, J. and Levy, Y. (2017) On the Coupling between the Dynamics of Protein and Water. *Physical Chemistry Chemical Physics*, **19**, 8243-8257. https://doi.org/10.1039/C6CP07669F

[11] Biswal, H.S., Loquais, Y., Tardivel, B., Gloaguen, E. and Mons, M. (2011) Isolated Monohydrates of a Model Peptide Chain: Effect of a First Water Molecule on the Secondary Structure of a Capped Phenylalanine. *Journal of American Chemical Society*, **133**, 3931-3942. https://doi.org/10.1021/ja108643p

[12] Lytkin, A.I., Krutova, O.N., Tyunina, E.Y., Chernikov, V.V., Mokhova, Y.V. and Krutova, E.D. (2021) Thermochemical Study of Reactions of Acid-Base Interaction in an L-Glutathione Aqueous Solution. *Russian Journal of Physical Chemistry A*, **95**, 2051-2054. https://doi.org/10.1134/S0036024421100162

[13] Lanza, G. and Chiacchio, M.A. (2016) Effects of Hydration on the Zwitterion Trialanine Conformation by Electronic Structure Theory. *Journal of Physical Chemistry B*, **120**, 11705-11719. https://doi.org/10.1021/acs.jpcb.6b08108

[14] Lapelosa, M. (2017) Free Energy of Binding and Mechanism of Interaction for the MEEVD-TPR2A Peptide-Protein Complex. *Journal of Chemical Theory and Computation*, **13**, 4514-4523. https://doi.org/10.1021/acs.jctc.7b00105

[15] Gale, A.G., Odbadrakh, T.T., Ball, B.T. and Shields, G.C. (2020) Water-Mediated Peptide Bond Formation in the Gas Phase: A Model Prebiotic Reaction. *Journal of Physical Chemistry A*, **124**, 4150-4159. https://doi.org/10.1021/acs.jpca.0c02906

[16] Lanza, G. and Chiacchio, M.A. (2018) Quantum Mechanics Study on Hydrophilic and Hydrophobic Interactions in the Trivaline—Water System. *Journal of Physical Chemistry B*, **122**, 4289-4298. https://doi.org/10.1021/acs.jpcb.8b00833

[17] Arsiccio, A. and Shea, J.E. (2021) Pressure Unfolding of Proteins: New Insights into the Role of Bound Water. *Journal of Physical Chemistry B*, **125**, 8431-8442. https://doi.org/10.1021/acs.jpcb.1c04398

[18] Fischer, K.C., Voss, J.M., Zhou, J. and Garand, E. (2018) Probing Solvation-Induced Structural Changes in Conformationally Flexible Peptides: IR Spectroscopy of $Gly_3H^+ \cdot (H_2O)$. *Journal of Physical Chemistry A*, **122**, 8213-8221. https://doi.org/10.1021/acs.jpca.8b07546

[19] Huggins, D.J. (2016) Studying the Role of Cooperative Hydration in Stabilizing Folded Protein States. *Journal of Structural Biology*, **196**, 394-406. https://doi.org/10.1016/j.jsb.2016.09.003

[20] Yu, H. and Rick, S.W. (2010) Free Energy, Entropy and Enthalpy of a Water Molecule in Various Protein Environments. *Journal of Physical Chemistry B*, **114**, 11522-11560. https://doi.org/10.1021/jp104209w

[21] Chalikian, T.V. (2021) Does the Release of Hydration Water Come with a Gibbs Energy Contribution? *Journal of Chemical Thermodynamics*, **158**, Article ID: 106409. https://doi.org/10.1016/j.jct.2021.106409

[22] Wachlmayr, J., Fläschner, G., Pluhackova, K., Sandtner, W., Siligan, C. and Horner, A. (2023) Entropic Barrier of Water Permeation through Single-File Channels. *Communications Chemistry*, **6**, Article No. 135. https://doi.org/10.1038/s42004-023-00919-0

[23] Cheatham, T., Darden, T., Gohlke, H., Luo, R., Merz Jr, K.M., Onufriev, A., Simmerling, C., Wang, B. and Woods, R. (2005) The Amber Biomolecular Simulation Programs. *The Journal of Computational Chemistry*, **26**, 1668-1688. https://onlinelibrary.wiley.com/doi/full/10.1002/jcc.20290

[24] (2002) Hyper Chem Professional 7.51. Hypercube, Inc., Gainesville. http://www.hypercubeusa.com/

[25] Frisch, M.J., Trucks, G.W., Schlegel, H.B., Scuseria, G.E., Robb, M.A., Cheeseman, J.R., Scalmani, G., Barone, V., Petersson, G.A., Nakatsuji, H., Li, X., Caricato, M., Marenich, A.V., Bloino, J., Janesko, B.G., Gomperts, R., Mennucci, B., Hratchian, H.P., Ortiz, J.V., Izmaylov, A.F., Sonnenberg, J.L., Williams-Young, D., Ding, F., Lipparini, F., Egidi, F., Goings, J., Peng, B., Petrone, A., Henderson, T., Ranasinghe, D., Zakrzewski, V.G., Gao, J., Rega, N., Zheng, G., Liang, W., Hada, M., Ehara, M., Toyota, K., Fukuda, R., Hasegawa, J., Ishida, M., Nakajima, T., Honda, Y., Kitao, O., Nakai, H., Vreven, T., Throssell, K., Montgomery, J.A., Peralta, J.E., Ogliaro, F., Bear-

park, M.J., Heyd, J.J., Brothers, E.N., Kudin, K.N., Staroverov, V.N., Keith, T.A., Kobayashi, R., Normand, J., Raghavachari, K., Rendell, A.P., Burant, J.C., Iyengar, S.S., Tomasi, J., Cossi, M., Millam, J.M., Klene, M., Adamo, C., Cammi, R., Ochterski, J.W., Martin, R.L., Morokuma, K., Farkas, O., Foresman, J.B. and Fox, D.J. (2016) Gaussian 16, Revision B.01. Gaussian, Inc., Wallingford. https://gaussian.com/gaussian16/

[26] McQuarrie, D.A. and Simon, J.H. (1997) Physical Chemistry: A Molecular Approach. University Science Books, Mill Valley. https://uscibooks.aip.org/books/physical-chemistry-a-molecular-approach/

[27] Malis, M., Loquais, Y., Gloaguen, E., Biswal, H.S., Piuzzi, F., Tardivel, B., Brenner, V., Broquier, M., Jouvet, C., Mons, M., Doslic, N. and Ljubic, I. (2012) Unraveling the Mechanisms of Nonradiative Deactivation in Model Peptides following Photoexcitation of a Phenylalanine Residue. *Journal of American Chemical Society*, **134**, 20340-20351. https://doi.org/10.1021/ja3054942

[28] Malis, M. and Doslic, N. (2017) Nonradiative Relaxation Mechanisms of UV Excited Phenylalanine Residues: A Comparative Computational Study. *Molecules*, **2**, Article 493. https://doi.org/10.3390/molecules22030493

[29] Alauddin, M. (2021) Effect of Solvents and Temperature on the Structural, Thermodynamic and Electronic Properties of Capped Phenylalanine: A Computational Study. *Journal of Bangladesh Academy of Sciences*, **45**, 205-215. https://doi.org/10.3329/jbas.v45i2.57212

[30] Alauddin, M. and Ripa, J.D. (2022) Effect of Microhydration on the Peptide Backbone of N-Acetyl-Phenylalaninylamide (NAPA) Using IR, Raman and Vibrational Chiroptical Spectrosocpies (VCD, ROA): A Computational Study. *European Journal of Applied Sciences*, **10**, 617-638. https://doi.org/10.14738/aivp.104.12859

[31] Alauddin, M. and Ripa, J.D. (2023) A TD-DFT Study for the Excited State Calculations of Microhydration of N-Acetyl-Phenylalaninylamide (NAPA). *Computational Chemistry*, **11**, 37-52. https://doi.org/10.4236/cc.2023.112003

[32] Gao, A., Li, G., Peng, B., Weidman, J.D., Xie, Y. and Schaefer III, H.F. (2020) The Water Trimer Reaction OH + $(H_2O)_3$ → $(H_2O)_2OH$ + H_2O. *Physical Chemistry Chemical Physics*, **22**, 9767-9774. https://doi.org/10.1039/D0CP01418D

[33] Lanza, G. and Chiacchio, M.A. (2017) Quantum Mechanics Approach to Hydration Energies and Structures of Alanine and Dialanine. *ChemPhysChem*, **18**, 1586-1596. https://doi.org/10.1002/cphc.201700149